



## Experimental investigation of fibre reinforced plastics with hybrid layups under high-velocity impact loads

Marco Romano, Carl J. J. Hoinkes, Ingo Ehrlich

*Ostbayerische Technische Hochschule Regensburg, Department of Mechanical Engineering, Laboratory of Composite Technology, Galgenbergstrasse 30, 93053 Regensburg, Germany*

Johann Höcherl

*University of the Bundeswehr Munich, Department of Mechanical Engineering, Laboratory of Ballistics, Arms and Munitions, Werner-Heisenberg-Weg 39, 85577 Neubiberg, Germany*

Norbert Gebbeken

*University of the Bundeswehr Munich, Department of Civil Engineering and Environmental Sciences, Institute of Engineering Mechanics and Structural Analysis, Werner-Heisenberg-Weg 39, 85577 Neubiberg, Germany*

**ABSTRACT.** This paper deals with experimental investigations concerning energy dissipation capacity of different kinds of reinforcement fibres in monolithic and hybrid layups under high-velocity impact loads. The investigated kinds of fibres are carbon, glass and basalt fibres. Therefore test panels, using the same thermoset resin, were built up and cured by autoclave processing. The fibre volume content of the test panels has been determined. Furthermore the influence of a separating layer at selected positions in the hybrid stacked panels was investigated. The results show the influence and the energy dissipation capacity of each single kind of fibre and the enhanced properties for the hybrid layups by hybrid stacking sequences and the use of a separating core material.

**SOMMARIO.** In questo lavoro le capacità di dissipazione dell'energia cinetica sotto carico trasversale ad alta velocità di materiali polimerici rinforzati con fibre sono state studiate mediante prove sperimentali. Le costruzioni delle piastre sono monolitiche ed ibride con e senza strato separante. I materiali di fibra usati in dettaglio sono carbonio, vetro e basalto, ciascuno come tessuto spigato con una tessitura 2/2. I materiali sono stati impregnati con la stessa matrice termoidurente e curati con un'autoclave. I contenuti di fibra sono stati determinati sperimentalmente. In oltre l'effetto di uno strato separante ad una posizione selezionata nella costruzione delle piastre ibride è stato identificato. I risultati mostrano l'effetto e la capacità di dissipazione dell'energia cinetica a causa di penetrazione per ogni tipo di fibra rinforzante e le maggiori proprietà delle costruzioni ibride con e senza strato separante.

**KEYWORDS.** Fibre reinforced plastic; High-velocity impact; Energy dissipation; Hybrid stacking.



## INTRODUCTION

Fibre reinforced plastics are increasingly applied in the automotive sector as well as for personal impact protection issues. Thereby especially the crash behavior and the failure mechanisms have to be researched properly in order to ensure safety for car passengers and facilitate recovery in the crash case. Fibre reinforced plastics consisting of only one kind of reinforcement fibres under high-velocity impact loads mostly fail in a brittle failure mode causing sharp-edged fracture surfaces and splitters.

In order to use the outstanding properties of each single kind of fibre and to avoid the afore-mentioned brittle failure modes to an optimum, the idea of using hybrid stacking sequences is adequate. Under these conditions fibre reinforced plastics with hybrid stacking sequences can be used as load-bearing structures and at the same time as safety structure for passengers in automotive or aerospace applications. Moreover, with the hybrid stacked composites lightweight concepts can efficiently be realized regarding energy saving issues.

## RESEARCH ENVIRONMENT

The research environment is the material behavior of fibre reinforced plastics under transversal loads in the high-velocity range. Therefore a brief literature review is presented. This leads to several conclusions and to the pursued mechanical principle described thereafter.

### *Literature review*

Energy dissipation mechanisms in fibre reinforced plastics are dominated by inter- and intralaminar failure modes as well as adhesive failure in the interface between fibre and matrix. Whereas interlaminar failure means the delamination of sequent plies, intralaminar failure means fracture of fibre and matrix. Only a small amount of energy is dissipated by friction effects between fibre and matrix and plastic deformation in the polymeric matrix system. Different material parameters affect the failure modes. These are amongst others fibre orientation, fibre volume content, layup, geometry of the specimen and of the impactor as well.

Maier 1990 [7] investigated the crash-behavior of tubular specimens with different cross-sections by experiments and finite-element-analyses. The specimens were made of glass fibre reinforced vinyl ester, poly ester and epoxy matrix system. The specimens with the epoxy matrix systems exhibited the highest energy dissipation capacity. Additionally the influence of the processing and the geometry on the energy dissipation capacity has been investigated.

Morita et al. 1997 [9] characterized the damage tolerance of fibre reinforced plastics under high-velocity impact loads with a varied degree of anisotropy. Thereby the degree of anisotropy means the change of fibre orientation for sequent layers in the layup. The results showed an enhanced energy dissipation capacity with an increased degree of anisotropy for sequent layers in the layup. Simultaneously the damage area in terms of interlaminar delaminations increased.

Holmquist and Johnson 2002 and 2005 [5, 4] investigated the reaction of silicone carbide to transversal impact loads in the high-velocity range. The investigated material is a ceramic. The originally high energy dissipation capacity could even be enhanced by creating predefined residual stresses, suited to the specific material properties.

Muhi, Najim and Moura. 2009 [11] considered the effect of hybridization of glass fibre reinforced plastics with single layers of aramid fabrics under transversal high-velocity impact. Therefore five kinds of different layups have been investigated experimentally. These are a monolithic layup consisting of only four layers of glass fabrics and in comparison four hybrid layups where at different positions in the layup one layer of glass fabric is substituted by one layer of aramid fabric (Kevlar 29) at a time. Additionally three different geometries of the impactor have been used. As a completion analytical approaches following Morye et al. 2000 [10] have been carried out. The hybridization in terms of substituting one layer of glass fabric with one layer of aramid fabric yields enhanced penetration resistance as well as sensitivity to the position of the hybrid substitute layer in the construction of the layup. In detail the hybridized layup where the opposite impact side has been substituted exhibits the highest energy dissipation properties.

Fadhel 2011 [3] carried out finite-element-analyses for pure polycarbonate specimens under high-velocity impact-loads varying their thickness. Additionally two different geometries of the impactor have been investigated. Even though the work is focused on pure polymeric materials the essential conclusion of the simulations is that an enhanced elastic sag could be identified as the main reason for an increasing dissipated energy.

Melo and Villena 2012 [8] investigated the influence of the fibre volume content on the energy dissipation capacity of fibre reinforced plastics. For glass fibre reinforced plastics with epoxy, polyester and vinyl ester matrix systems higher



values of the fibre volume content in the specimens yield significant higher energy dissipation properties. Additionally the materials with epoxy matrix system exhibited the highest energy dissipation capacity.

Rosenberg and Dekel 2012 [21] basically describe the experimental setup and procedure as well as the evaluation of the experimentally determined results when transversal impact-tests in the high-velocity range are described.

#### *Pursued mechanical principle*

The object in the carried out investigations is the identification of the energy dissipation capacity of fibre reinforced plastics under high-velocity impact loads. Thereby besides monolithic layups selected hybrid layups with and without separating layer are investigated. The aim is to enhance the energy dissipation capacities by hybrid layups based on fabrics of different kinds of fibre reinforcements besides using the outstanding material properties of fibre reinforced plastics as load bearing structures. Therefore two basic ideas are followed.

#### *Hybrid stacking sequences*

As a first approach the use of hybrid stacked layups instead of monolithic layups is relatively simple. Thereby the characteristic properties of carbon and glass fibres, completed by basalt fibres, respectively, can be used through the thickness in by reasonably defined hybrid stacking sequences. Aramid fibres have not been considered, because of their distinct hygroscopicity and resulting in difficulties when being impregnated as described later on.

#### *Separating layer as elastic support*

A second approach is the use of separating layers as a core material. Here, especially relatively thin separating layers with relatively low stiffness are used. In the present application, however, it is not used with the aim of enhancing the moment of inertia as usually done. In contrast the used separating layers with the afore described properties provide an elastic support and a shear plane for the single layers in the layup. Thereby transversal loads can increasingly be transferred to in-plane loads.

This effect is reached by additionally providing transversal deflection due to shear effects and therewith enhances the resulting in-plane loads in the material [6]. The reason for this pursued principle is, that fibre reinforced plastics show its outstanding properties under in-plane tensile loads in direction of the reinforcement fibres. The aim is to reduce the effect of simply stamping the material by the impactor but enable the afore described structural mechanic effects similarly to Fadhel 2011 [3].

#### *Limit of the experimental investigations*

With the afore described basic ideas the initial situation for using the light-weight properties of fibre reinforced plastics as well as enhance their resistance to transversal impact loads in the high-velocity range can be created. These two basically different properties enable the application of fibre reinforced plastics as load-bearing structure and at the same time as protective structure. If thereby for load-bearing structures additional protective structures can be omitted, a holistic light-weight approach can be achieved.

Alternative approaches for enhancing the resistance of fibre reinforced plastics under transversal impacts in high-velocity range by the impact resistance of the matrix, i.e. by definably adding small amounts of thermoplastics in the thermoset matrix system is not the aim of the carried out investigations. They are merely focused on the material suited or fibre suited application of different kinds of reinforcement fibres in hybrid stacked layups, respectively.

#### *General experimental conditions*

Knowing that different layer orientations have influence on the energy dissipation capacity [9] all test panels have been built up with a  $[(0/90)_n]$  orientation. This was done as a first attempt for characterizing the general material behavior. The fibre volume content is a significant parameter for the quality and reproducibility of fibre reinforced plastics [6], [24], [25]. Moreover it has a massive influence on the energy dissipation capacity [8].

In order to experimentally investigate the specific capacities of monolithic and hybrid stacking sequences regarding energy dissipation high-velocity impact tests with an impact velocity of approx. 560 m/s have been carried out. Thereby bearing balls have been used as an impactor. With a mass of approx. 1.12 g the initial kinetic energy before the impact lies in the range of 175 J. The reason therefore is that the spheric bearing balls are insensitive to variations in the angle of incidence. In contrast cylindrical blunt-ended or conical projectiles would cause distinct stress peaks in the specimen. This is due to variations of the angle of incidence caused by statistic deviations. Analog observations have been made e. g. by Muhi, Najim and Moura. 2009 [11]. It is additionally observed that the selected spheric geometry provides reasonable values for the energy dissipation properties [11].

Evaluation of the experimentally obtained results for the velocities of the impactor before and after the penetration according to [21] provides information about the capacity for each single stacking sequence to dissipate kinematic energy.

## MATERIALS AND TEST PROCEDURES

In the following the used materials and the material processing is described. The used experimental equipment to determine the fibre volume content and the energy dissipation capacity are mentioned. The respective standards (DIN, EN or ISO) are indicated.

### Materials and processing

For the processing of the test panels three different kinds of fabrics and one core material have been used. Tab. 1 contains the fabrics used for the production of test panels and the core material.

The tested hexagonal core material is of the kind LANTOR SORIC XF [19] with a thickness of approx. 4 mm. It is used as a hexagonal separating layer. This separating layer aims at an enhanced sag of the test panels [6], which should dissipate more energy when penetrated [3].

Three kinds of reinforcement fibres have been used. In each case a twill weave 2/2 has been used as a textile semi-finished product for further processing and building-up the selected layups.

In order to achieve a statistically secured amount of comparable specimens five test panels have been produced for each selected layup. Therefore the single fabric reinforced layers have manually been pre-impregnated. This process enables the choice of the selected thermoset resin EPIKOTE RESIN 04572 [17] as a matrix system for all produced test panels. The curing was done in an autoclave process under a vacuum bag according to the process indicated in the data sheet of the matrix system EPIKOTE RESIN 04572 [17].

Kind of fibre	Type of fabric	Spec. weight [g/m <sup>2</sup> ]	Warp [1/cm]	Fill [1/cm]	Literature
Carbon	twill 2/2	245	6	6	[13]
Glass	twill 2/2	280	7	6.5	[18]
Basalt	twill 2/2	345	12	9	[12]
Hexagonal Core Mat.	-	240	-	-	[19]

Table 1: Types of fabrics and core material.

With these parameters a panel thickness of approx. 4 mm and a fibre volume content of approx. 60 % have been achieved. In order to reach a constant thickness of the test panels the number of single layers in each layup has to be adopted due to the varying thicknesses of the fabrics. Fig. 1 left shows the scheme of the used processing layup considering the vacuum bag in the autoclave curing process. Fig. 1 right shows the corresponding autoclave curing cycle in terms of temperature  $T$  in °C, relative pressure  $p$  in bar, and relative vacuum in bar over the process time  $t$  in min.

The geometric dimensions have been selected following DIN 65561 [14]. The German standard requires a final lateral geometry of the specimens of 150 mm x 100 mm. The panels have been built up with a dimension of 210 mm x 160 mm since the edges of the test panels become inhomogeneous and unsteady. The edges have then been cut off by water jet cutting. Specimens for the experimental determination of the fibre volume content  $\varphi_f$  have been cut off from the cut-off regions near the cutting edge. Their dimensions are approx. 15 mm x 15 mm according to DIN EN ISO 1172 [15] and DIN EN 2564 [16], respectively. Fig. 2 shows schematic the layup and the cutting lines for test panels and the specimen for fibre volume content determination.

Tab. 2 lists the investigated types of test panels with their respective labeling, stacking sequence and number of single layers. Thereby five test panels have been produced for every single type, so that 25 specimens have been investigated. There are three kinds of monolithic layups consisting of only carbon, glass and basalt fabric reinforced layers. Additionally there are two kinds of hybrid layups consisting of carbon, glass and basalt. They distinguish from each other by an additionally added hexagonal separating layer LANTOR SORIC XF [19] as a core material after the first twelve fabrics or before the last four fabrics, respectively, considering the direction of the later impact.

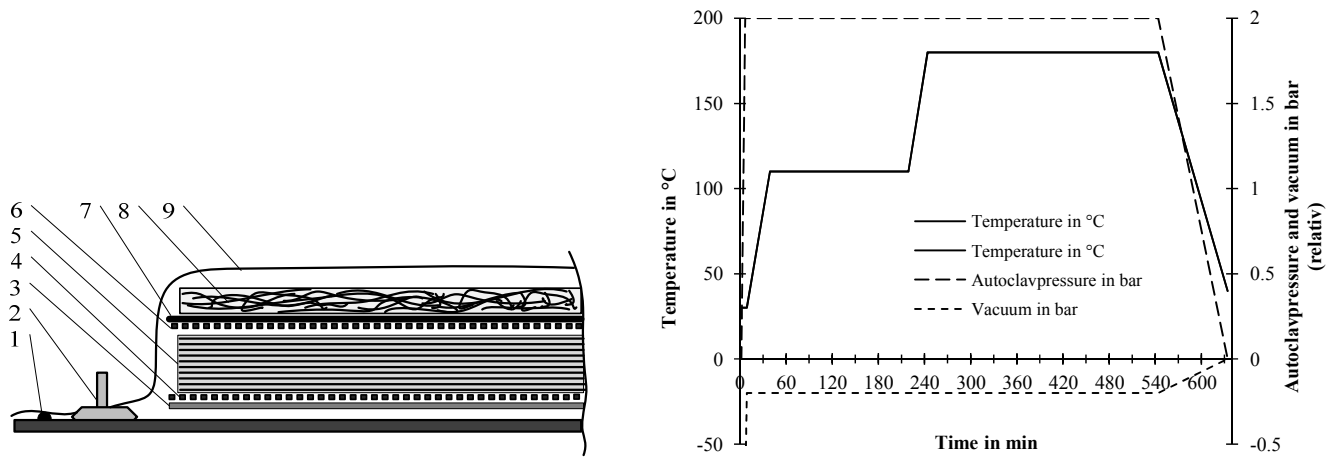


Figure 1: Left: Scheme of the layup used in the processing: 1 sealant tape, 2 vacuum connector, 3 release film, 4 peel ply, 5 composite layup, 6 peel ply, 7 perforated foil, 8 bleeder, 9 vacuum bag. Right: Autoclave curing cycle for test panel processing in terms of temperature  $T$  in °C, relative pressure  $p$  in bar, and relative vacuum in bar over the process time  $t$  in min.

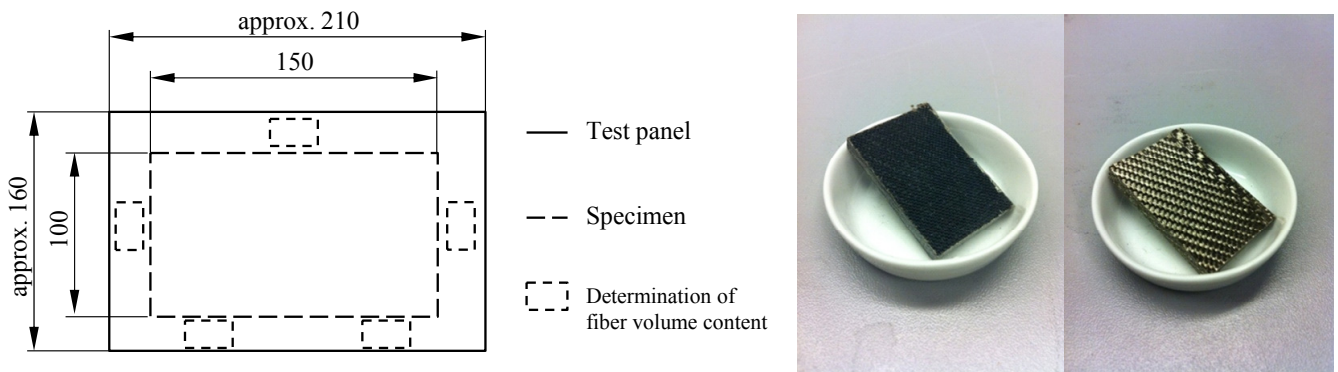


Figure 2: Schematic cutting lines for test panels and fibre volume content specimens (left) and exemplary specimens for basalt fibre reinforced material before and after the thermal treatment according to DIN EN ISO 1172 [15], [23] (right).

Type of test panel	Stacking sequence	Number of Layers
Carbon	$[0/90]_{18}^C$	18
Glass	$[0/90]_{18}^G$	18
Basalt	$[0/90]_{18}^B$	18
C+G+B	$[(0/90)_4^C / (0/90)_4^G / (0/90)_8^B]$	16
C+G+Hex+B	$[(0/90)_4^C / (0/90)_4^G / (0/90)_4^B / (Hex)_1 / (0/90)_4^B]$	16+1

Table 2: Labeling, stacking sequences and number of layers of the test panels.



### *Experimental determination of the fibre volume content*

Basically there are two methods for experimentally investigating the fibre volume content. Whereas for inorganic fibres like glass or basalt fibres it can be determined by thermal vaporization the polymeric matrix system according to DIN EN ISO 1172 [15], [23], for organic fibres like carbon fibres it can be determined by chemical extraction of the fibres according to DIN EN 2564 [16]. For a statistically ensured determination five specimens of every test panel with geometric dimensions of approx. 15 x 15 mm have been investigated. In both cases knowing the mass of the initial specimen and the remaining fibres as well as the densities of the single components, namely fibre and matrix, it is possible to determine the fibre volume content  $\phi_f$ . In the following the two afore mentioned experimental methods are described.

### *Thermal vaporization of the polymeric matrix system according to DIN EN ISO 1172*

For the panels that contain only glass or basalt fibres as inorganic reinforcement fibres the fibre volume content  $\phi_f$  can be determined experimentally using a muffle furnace and a precision balance following DIN EN ISO 1172 [15]. The furnace is of the type CARBOLITE EML 11/6, required to reach the temperature of 620 °C. This temperature is necessary to evaporate the polymeric matrix without affecting the mass of the fibres [2], [22], [23], [24]. The precision balance is of the type METTLER TOLEDO 204-S being able to supply an accuracy of measurements in a range of 0.1 mg. With the precision balance it is possible to weigh the specimens before and the remaining fibres after the thermal treatment and so determining the fibre volume content  $\phi_f$ .

### *Chemical extraction of the fibres according to DIN EN 2564*

The afore described process is not suitable for carbon fibres. These kinds of reinforcement fibres show a distinct loss of weight under thermal loads [1], [24] as they are of organic structure. Therefore the process of chemical extraction was used for test panels that only contain carbon fibres following DIN EN 2564 [16]. The fibres are extracted from the matrix by placing the specimens in concentrated sulphuric acid and heating up to 160 °C. After the solution turns brown, hydrogen peroxide solution is added until the solution turns clear again. This effect is an indicator that the fibres have been completely extracted from the matrix. Redrying wet fibres enables weighing them and thereby the calculation of the fibre volume content  $\phi_f$ .

### *Evaluation of the results and calculation of the fibre volume content*

As previously described, the specimens have been weighted before and the remaining fibres after the respective treatment. Knowing these weights the fibre mass content can be calculated by

$$\psi = \frac{m_f}{m_c} \quad (1)$$

where  $m$  indicates the mass and the subscripts  $f$  and  $c$  indicate the properties of the fibres and of the composite, respectively. Knowing the fibre mass content  $\psi$  and the densities of the single components, namely reinforcement fibres and polymeric matrix system, out of the respective technical data sheets [12, 13, 17, 18] the fibre volume content can be calculated by

$$\phi_f = \frac{1}{1 + \frac{1-\psi}{\psi} \cdot \frac{\rho_f}{\rho_m}} \quad (2)$$

where  $\rho$  is the density,  $\psi$  is the fibre mass content and the subscripts  $f$  and  $m$  indicate the properties of the fibre and the matrix, respectively [6], [24].

### *Analytical approximation of fibre volume content for test panels with hybrid stacking sequences*

When the hybrid stacked layups are considered none of the two afore described experimental methods for the determination of the fibre volume content are suitable because both organic and inorganic kinds of reinforcement fibres are used in the respective layups, as listed in Tab. 3. Neither the thermal vaporization method according to DIN EN ISO 1172 [15] nor the chemical extraction method according to DIN EN 2564 [16] is applicable.

Therefore an approximation method has been developed in order to being able to analytically evaluate the fibre volume content of the hybrid stacked layups. The approximation is based on the specific weights of the dry fabrics and the weight of the prepared specimens. The mass of the fabrics in the specimen can be calculated by



$$m_f = A \sum_{i=1}^m (Q_i \cdot n_i) \tag{3}$$

where  $m$  is the mass,  $A$  is the area of the test panel,  $Q$  is the specific weight of the fabric,  $n$  is the number of the single layers of each fabric and the subscript  $f$  indicates the property of all fabrics in the layup. Considering the summation  $i$  is the counter for the different kinds of reinforcement fibres used and  $m$  is the upper limit of the counter, i. e. the number of the different kinds of reinforcement fibres used in the hybrid stacked material.

The mass of the composite  $m_c$  is obtained by weighing the single specimens on a precision balance. The fibre mass content in the specimen  $\psi$  can then be calculated by evaluating Eq. (1).

For an analytical evaluation of the fibre volume content  $\phi_f$  the density of the fibres  $\rho_f$  is necessary. Because more than one kind of reinforcement fibre is used in the hybrid stacked materials the fibre density is not a uniform value for the material. Yet it is possible to analytically evaluate a mean value of the density of the fibre reinforcement in the composite material  $\bar{\rho}_f$ . Therefore the volume of each kind of dry fabrics is calculated by

$$V_i = A \cdot t \cdot n_i \tag{4}$$

where  $A$  is the area of the specimen,  $n$  is the number of the single layers of each fabric,  $i$  is the counter for the different kinds of reinforcement fibres used and  $t$  is the thickness of each single fabric reinforced layers. Thereby the values of the thickness of the single fabric reinforced layers have been taken from the respective technical data sheets [12], [13] and [18]. The mean value of the density of the fibre reinforcement in the composite material is analytically calculated by

$$\bar{\rho}_f = \frac{\sum_{i=1}^m (V_{f,i} \cdot \rho_{f,i})}{\sum_{i=1}^3 V_{f,i}} \tag{5}$$

where  $V$  is the volume of each kind of dry fabrics,  $\rho$  is the nominal density of each kind of reinforcement fibre and the subscript  $f$  indicates the property of the fabric reinforcement. Considering the summation  $i$  is the counter for the different kinds of reinforcement fibres used and  $m$  is the upper limit of the counter, i.e. the number of the different kinds of reinforcement fibres used in the hybrid stacked material.

Type of test panel	Mean value $\phi_f$ (%)	Standard deviation $\phi_f$ (%)
Carbon	63.60	0.46
Glass	58.65	0.94
Basalt	61.16	0.66
C+G+B	63.07	0.72
C+G+Hex+B	57.15	1.36

Table 3: Fibre volume contents of the test panels.

The calculation of the fibre volume content according to Eq. (2) can be carried out by using the mean value of the density of the fibre reinforcement in the composite material  $\bar{\rho}_f$  instead of the density of a single kind of reinforcement fibre  $\rho$ . Though, it is sufficient to average the density of the used fibre reinforcement and carry out the evaluation according to Eq. (5).

### Resulting values for the fibre volume content $\phi_f$ obtained by the different applied methods

The results of the fibre volume content of the single layups are listed in Tab. 3 with its mean values and corresponding standard deviations. The relatively high values of the fibre volume content show high mechanical quality of the material. The relatively low standard deviations represent a high degree of reproducibility of the process at the same time.

### Experimental setup for high-velocity impact tests

In order to carry out and properly evaluate high-velocity impact tests an adequate experimental setup of test equipment is necessary. The experimental setup is schematically shown in Fig. 3 left. It consists of

- an instrumented barrel for acceleration of the impactor on the target,
- two photoelectric barriers for measuring the velocity of the impactor before the impact,
- a test panel mounting where the specimens are inserted and clamped all around with eight bolts M8, each tightened with 5 Nm,
- a double exposure instrumentation with the respective high-speed photographic camera for measuring the velocity of the Impactor after penetration of the target and
- a bullet screen and a fire case for absorbing the impactor and fragments that have eventually been released.

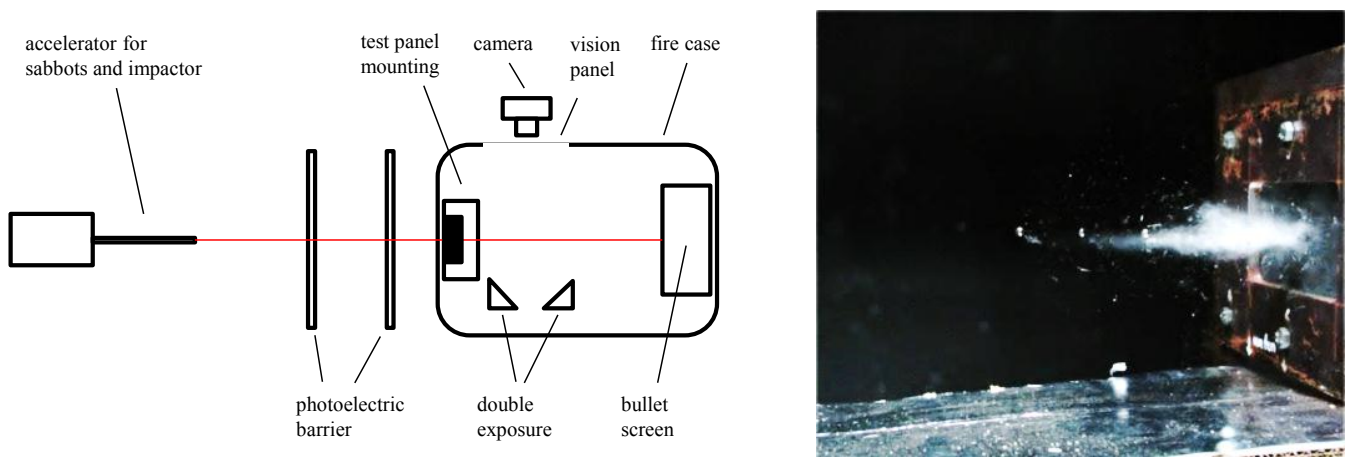


Figure 3: Schematic illustration of the experimental setup for high-velocity impact tests (left) and high-speed image of the debris after penetration under double exposure (right).

The bearing balls are of the steel type 100Cr6. With a diameter of 6.5 mm and the corresponding density of 7.61 g/cm<sup>3</sup> the impactors have a mass of  $1.12 \pm 0.0005$  g. Computer numerically controlled (CNC) manufactured plastic sabots were used to accelerate the bearing balls in a barrel. The case on which the plastic sabot is mounted is filled with a special propellant, which was weighted to 0.1 mg precision in order to properly accelerate the impactor in the barrel after ignition. The aforescribed procedure provides reproducible velocities of the impactor after having left the barrel [21].

On the ballistic flight of the impactor the photoelectric barrier provides the velocity of the impactor before the impact  $v_1$ , the impactor hits the target and after penetration the double exposure with the high-speed camera provides the velocity of the impactor after the penetration  $v_2$ . Fig. 3 right exemplarily shows an image of the high-speed camera after the impactor has penetrated the material. Due to the double exposure the impactor is pictured twice. Knowing the time between the two exposures measuring the distance between the two pictured impactors on the image allows the calculation of the velocity of the impactor after the penetration  $v_2$ .

The design of the plastic sabots exhibits four defined slots in longitudinal direction. These slots guarantee the bulking of the plastic sabot after having left the barrel whereas the bearing ball continues its ballistic flight nearly straightly and at constant speed. With the specific design of the plastic sabots the impact of fragments of the plastic sabot in the area of the specimen can be excluded. Fig. 4 left shows the manufactured plastic sabots made of the material POM [20] with the mounted case. Fig. 4 right exemplarily shows a high-speed image of the bulking of the plastic sabot after having left the barrel.



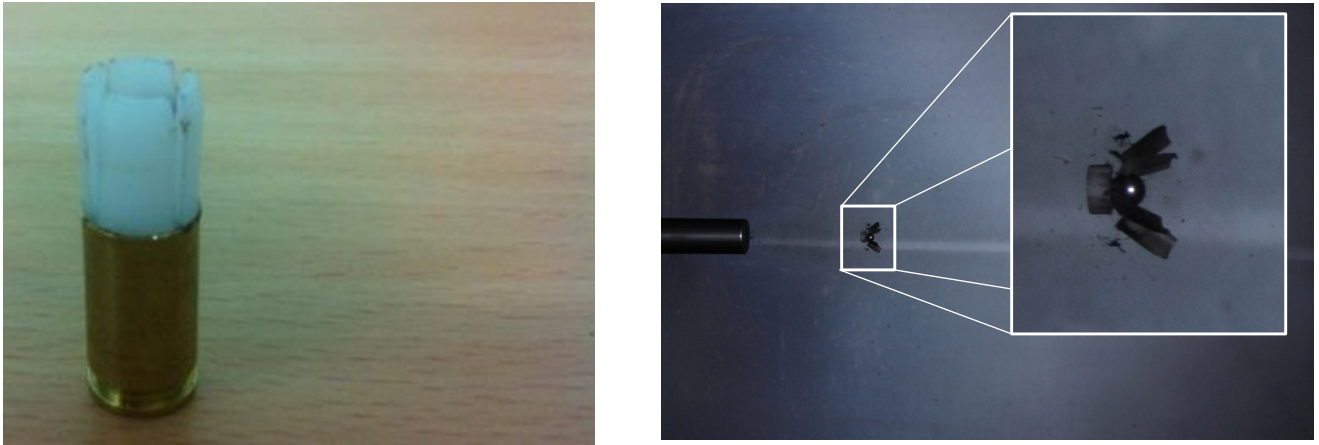


Figure 4: CNC-manufactured plastic sabots with the mounted case containing precisely weighted propellant (left) and high-speed image of the bulking of the plastic sabot after having left the barrel whereas the bearing ball continues its undisturbed ballistic flight (right).

## RESULTS AND DISCUSSION

In the following the evaluation of the experimental results is described. The obtained results are discussed and lead back to acting effects.

### *Evaluation of experimental results*

For the evaluation of the experimental investigation each bearing ball is weighted to 0.1 mg precision. The mass of the impactors  $m$  lie in the range of  $1.12 \pm 0.0005$  g. Knowing the velocity of the impactor before the impact provided by the photoelectric barrier  $v_1$  and the velocity of the impactor after penetration of the material provided by the double exposure and the high-speed camera  $v_2$  the kinetic energy for both states can be calculated by

$$E_{\text{kin},n} = \frac{1}{2} m v_n^2 \quad (6)$$

where  $m$  is the mass,  $v$  is the velocity and  $n$  indicates the states, 1 before and 2 after the penetration of the material [21]. The mean value of the velocity of the impactor before the impact  $v_1$  lies in the range of  $560.3 \pm 5.8 \text{ m/s}$  and the respective kinetic energy before the impact  $E_{\text{kin},1}$  lies in the range of  $175.8 \pm 3.7$  J. The difference between the kinetic energies before the impact  $E_{\text{kin},1}$  and after the penetration of the material  $E_{\text{kin},2}$  allows calculating the absolute value for the dissipated energy by penetrating the material by [21]

$$E_{\text{diss}} = \Delta E_{\text{kin}} = E_{\text{kin},1} - E_{\text{kin},2} = \frac{1}{2} m (v_1^2 - v_2^2) \quad (7)$$

In order to properly evaluate each single test and achieve nondimensional comparable results for the carried out experimental investigations it is reasonable to introduce the relative dissipated kinetic energy [21]

$$E_{\text{diss,rel}} = \frac{\Delta E_{\text{kin}}}{E_{\text{kin},1}} = \frac{\frac{1}{2} m (v_1^2 - v_2^2)}{\frac{1}{2} m v_1^2} = \frac{v_1^2 - v_2^2}{v_1^2} = 1 - \frac{v_2^2}{v_1^2} \quad (8)$$

where the dissipated kinetic energy due to penetration of the material  $\Delta E_{\text{kin}}$  is related to the initial kinetic energy of the Impactor  $E_{\text{kin},1}$ . The introduction of the relative dissipated kinetic energy  $E_{\text{diss,rel}}$  provides a specific value in percent. It

indicates the capacity of a material to dissipate kinetic energy applied by high-velocity impacts when the material gets penetrated.

The experimentally determined fibre volume contents  $\phi_f$  vary in a range of 63 % to 57 %. The distinct variation exists even though the same manufacturing process described before as well as the same autoclave curing cycle illustrated in Fig. 1 right has been used. That is the reason why the former described evaluation of the relative dissipated kinetic energy  $E_{\text{diss,rel}}$  has to be evaluated additionally. In order to standardize the further calculated values based on the nominal values a standardization of the relative dissipated kinetic energy  $E_{\text{diss,rel}}$  to a constantly presumed fibre volume content  $\phi_{f,s}$  is carried out by calculating

$$E_{\text{diss,rel}}(\phi_{f,s}) = E_{\text{diss,rel}} \frac{\phi_{f,s}}{\phi_{f,e}} \quad (9)$$

where the subscripts  $s$  and  $e$  indicate the desired standardized value for the fibre volume content and the experimentally determined fibre volume content listed in Tab. 3, respectively. As already mentioned before the autoclave curing cycle was modified in order to achieve a fibre volume content of approx. 60 %. Therefore the presumed fibre volume content for the standardization is selected to  $\phi_{f,s} = 60\%$ .

### Results

The results are illustrated in terms of the relative dissipated energy of the materials based on the nominal values of the fibre volume content  $\phi_{f,e}$  as well as standardized to the desired value of the fibre volume content  $\phi_{f,s} = 60\%$ .

Because five test panels of each selected layup have been investigated experimentally, the evaluation of the experimental results allows statistically assured results by calculating mean value and standard deviation for each material. As it can later be seen, the standard deviations are generally very low. This is an indicator for constant material quality for all the investigated test panels provided by the manufacturing process as well as for the high reproducibility of the experimental investigations of high-velocity impact loads.

#### Results based on the nominal values of the fibre volume content $\phi_{f,e}$

Fig. 5 illustrates the relative dissipated kinetic energy  $E_{\text{diss,rel}}$  for each selected type of layup calculated by Eq. (8) for the three monolithic layups and for the hybrid stacking sequences with and without the hexagonal separating layer.

The relative dissipated kinetic energy of the test panels consisting of monolithic layups containing only a single kind of reinforcement fibre, illustrated in Fig. 5, range from 34 % to 44 %. The highest value of the relative dissipated kinetic energy of approx. 44 % is obtained for the test panels built up of only basalt fabrics. The test panels consisting of only glass fabrics dissipated approx. 37 % whereas the test panels containing only carbon fabrics dissipated approx. 34 % of the initial impact energy. The standard deviation is persistently low and lies in a range of 0.85 % to 2.2 %. Thereby the carbon fibre reinforced test panels showed the lowest standard deviation in contrast to the basalt fibre reinforced specimens that showed the highest values of the standard deviation.

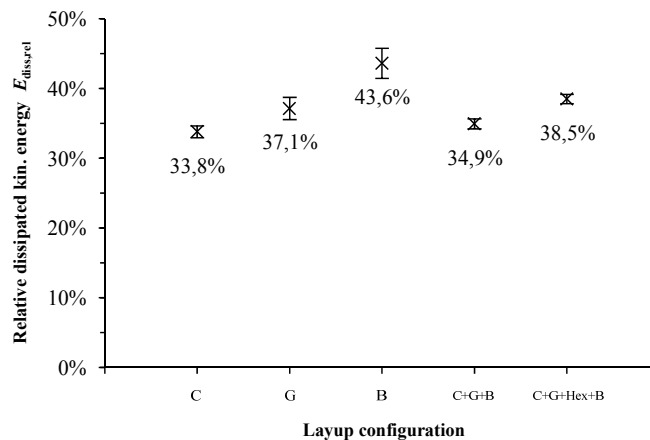


Figure 5: Relative dissipated kinetic energy  $E_{\text{diss,rel}}$  of the monolithic and hybrid materials based on the absolute values of the fibre volume content  $\phi_{f,e}$ .



The relative dissipated kinetic energy of the test panels consisting of the hybrid layups with and without the hexagonal separating layer range from 35 % to 39 %. Confronting the hybrid stacked layup without hexagonal separating layer and the hybrid stacked layup with hexagonal separating layer as a core material a distinct effect can be noticed. The hybrid stacked material with separating layer shows approx. 4 % higher values for the relative dissipated kinetic energy than the hybrid stacked layup without separating layer. In contrast to the monolithic materials the hybrid stacked materials showed the lowest standard deviation.

*Standardizing the results to a fibre volume content  $\phi_{f,s} = 60\%$*

Fig. 6 illustrates the relative dissipated kinetic energy  $E_{diss,rel}(\phi_{f,s} = 60\%)$  for each selected type of layup calculated by Eq. (9) as standardized results for the monolithic and hybrid layups with and without the hexagonal separating layer.

The relative dissipated kinetic energy  $E_{diss,rel}$  and the standardized relative dissipated kinetic energy  $E_{diss,rel}(\phi_{f,s})$  to desired value of the fibre volume content  $\phi_{f,s} = 60\%$  vary only slightly when the monolithic materials are considered. The standardized relative dissipated kinetic energy  $E_{diss,rel}(\phi_{f,s})$  of the monolithic materials, illustrated in Fig. 6, range from 32 % to 43 %. The highest value of the relative dissipated kinetic energy of approx. 43 % is still obtained for the test panels built up of only basalt fabrics. To the test panels consisting of only glass fabrics a value of approx. 38 % is assigned. For the monolithic carbon fibre reinforced layups the standardization yields a value of approx. 32 %. The standard deviations are standardized as well, so that the tendencies in the results based on the nominal values do not change.

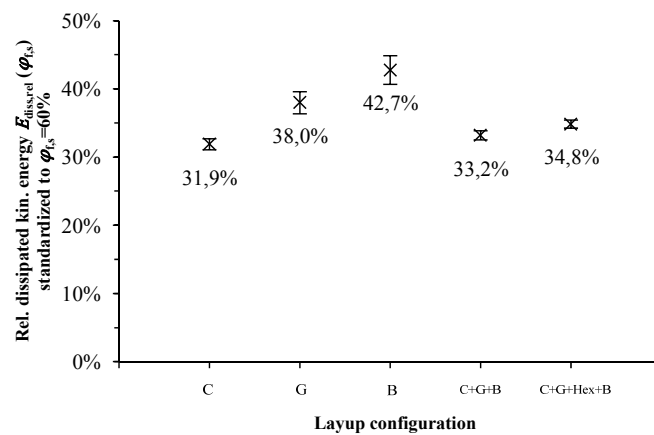


Figure 6: Relative dissipated kinetic energy  $E_{diss,rel}(\phi_{f,s})$  of the monolithic and hybrid materials standardized to a fibre volume content  $\phi_{f,s} = 60\%$ .

The relative dissipated kinetic energy  $E_{diss,rel}$  and the standardized relative dissipated kinetic energy  $E_{diss,rel}(\phi_{f,s})$  to the desired value of the fibre volume content  $\phi_{f,s} = 60\%$  vary only slightly, too, when the hybrid stacked materials are considered. They range from 33 % to 35 %. Because the initial values of the fibre volume content  $\phi_{f,e}$  do not distinctly differ from the desired value of the fibre volume content  $\phi_{f,s} = 60\%$  the tendencies are similar to the results obtained for the nominal values. However, the effects caused by the separating layer used as a core material are a little less distinct, yet clearly observable. The hybrid stacked material with separating layer shows approx. 2 % higher values for the standardized relative dissipated kinetic energy than the hybrid stacked layup without separating layer. Because the standard deviations are standardized as well, the tendencies in the results based on the nominal values do not change, as already mentioned before.

*Description of failure modes – impact surface and outlet areas*

In the following the characteristic failure modes of the different kinds of layups are confronted with each other. Therefore the fractured surfaces of the impact side as well as of the opposite side are described. Fig. 7 exemplarily shows the

characteristic fractured surfaces of the penetrated specimen. Whereas the top row shows the fractured surfaces on the impact side the bottom row shows the fractured surfaces on the opposite side.

The specimens that only contain carbon fibres show a distinct contour due to the penetration on the impact side. The distinct contour can be interpreted as a die-cutting effect because of the relatively high stiffness of the carbon fibre reinforced material. On the opposite side a splinted surface due to brittle fracture can be observed. Due to the typical opaque property for carbon fibre reinforced plastics interlaminar delaminations are not visible yet existing.

In contrast for the glass fibre reinforced specimens the interlaminar delaminations are cognizable due to the transparency of both the fibres and the matrix system. On the opposite side of the impact a clearly outlined delamination area can be identified between the last two single layers. Comparing the delamination areas on the impact side to the area on the opposite side a conical spreading of the delamination areas through the thickness can be assumed. Due to the  $[(0/90)_n]$  layups with equilibrated twill fabrics and the rectangular form of the free part of the specimen in the test panel mounting the delamination has a slight rectangular shape, too. Furthermore the lateral dimensions of the delamination on the opposite side of the impact are approx. 28 mm x 25 mm. Because the visible delaminated area is considerably smaller than the free part of the specimen in the test panel mounting the assumption that the boundary conditions are negligible can be confirmed.

For the basalt fibre reinforced material the interlaminar delaminations are not clearly identifiable due to the opaque optical properties of basalt fibres. Confronted to the glass fibre reinforced material the interlaminar delaminations on the opposite side of the impact can slightly be discerned. Because of the slightly unbalanced construction of the basalt fabric the delamination on the opposite side of the impact is distinctly rectangular with lateral dimensions of approx. 25 mm x 15 mm.

The contour due to the penetration on the impact side of the hybrid layups without separating layer are similar to the contours of the specimens that only contain carbon fibre reinforcement. On the opposite side of the impact the basalt fabrics cause a fine extensive fractured surface. On the opposite side of the impact the interlaminar delamination between the last single layers of basalt fabrics can slightly be discerned.

Regarding the hybrid layups with separating layer the contour due to the penetration on the impact side is shaped like the ones of the hybrid layups without separating layer or the purely carbon fibre reinforced material. On the opposite side of the impact the hexagonal structure of the core material is slightly visible. The fractured area can be identified to be slightly smaller compared to the hybrid specimens without separating layer.

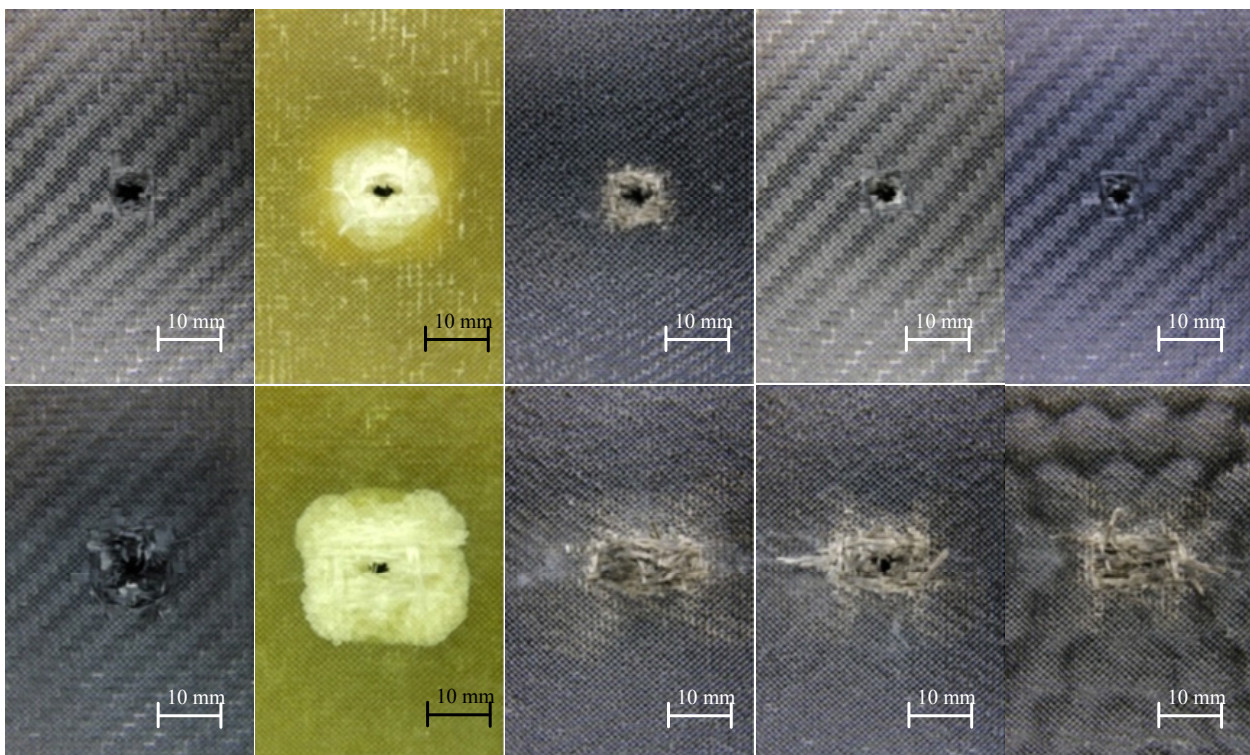


Figure 7: Characteristic failure modes of the different kinds of layups: From left to right: C (carbon), G (glass), B (basalt), C+G+B and C+G+Hex+B (Top row: Impact side, Bottom row: Opposite impact side).



## CONCLUSIONS

For all evaluated results the standard deviations are generally very low. This is an indicator for constant material quality for all the investigated test panels provided by the manufacturing process as well as for the high reproducibility of the experimental investigations of high-velocity impact loads.

The carried out high velocity impact tests showed the respective properties of each single kind of fibre when the monolithic layups have been considered. With a hybrid stacking it is possible to optimize the use of the outstanding material properties of each single kind of reinforcement fibres when energy dissipation issues under high-velocity impact loads are considered. Even though aramid fibres have not been considered as for example described in Muhi, Najim and Moura. 2009 [11] hybridization yields noticeable effects. The effect can directly be lead back to hybridization. The reasons therefore are the relatively high values of the fibre volume content  $\phi_{f,s} = 60\%$  and at the same time the relatively low standard deviations. These two indicators regarding the composite material imply a high mechanical quality as well as a high degree of reproducibility of the process at the same time. However, aramid fibres should be taken into account in further investigations as even a more distinct enhancement of the energy dissipation capacity can be expected.

The initially described idea to enhance transversal deflection due to shear effects and therewith enhance the resulting normal loads in the material can be identified in the evaluated results for the hybrid stacked materials with and without the hexagonal separating layers. The improved relative energy dissipation based on the nominal values as well as standardized to the desired fibre volume content distinctly proves the acting of the aimed structural mechanic effect. Thus, the functional capability of the layer as well as of the hybrid stacked layups can be stated. In further investigations different hybrid layups should be considered additionally. Thereby the focus should lie on the identification of the sensitivity of the energy dissipation properties to the sequential arrangement of the monolithic blocks in the construction of the hybrid stacked layups as basically carried out in Muhi, Najim and Moura. 2009 [11].

## ACKNOWLEDGEMENTS

The authors would like to thank Mr Marco Vogelsberg and Mr Uwe Riedel from the Laboratory of Ballistics, Weaponry and Munitions at the University of the Bundeswehr Munich as well as Mr Florian Roidl from the Laboratory of Manufacturing Engineering and Machine Tools (LFW) and Mr Bastian Jungbauer, B.Eng. from the Laboratory of Composite Technology (LFT), both at the Ostbayerische Technische Hochschule Regensburg.

Further Mrs Carmen Löpelt and Mr Elmar Lauterborn, both from the Wehrwissenschaftliches Institut für Werk- und Betriebsstoffe (WIWeB) Erding are gratefully acknowledged for carrying out the determination of the fibre volume content by chemical extraction.

The authors are grateful to the donation of the bearing balls from the company Schaeffler Technologies AG & Co. KG that have exhibited excellent properties as spheric impactors.

## REFERENCES

- [1] Cherif, C., *Textile Werkstoffe für den Leichtbau, Techniken-Verfahren-Materialien-Eigenschaften*. Springer-Verlag, Berlin/Heidelberg/New York, (2011).
- [2] Deak, T.; Czigany, T., *Chemical Composition and Mechanical Properties of Basalt and Glass Fibers: A Comparison*, *Textile Research Journal*, 79(7) (2009) 645-651.
- [3] Fadhel, B. M., *Numerically Study of Ballistic Impact of Polycarbonate*. International Symposium on Humanities, Science and Engineering Research (SHUSER), Kuala Lumpur, (2011) 101-105.
- [4] Holmquist, T., Johnson, G., *Characterization and evaluation of silicon carbide for high-velocity impact*, *Journal of Applied Physics*, 97 (2005) 1-12.
- [5] Holmquist, T., Johnson, G., *Response of silicon carbide to high velocity impact*, *Journal of Applied Physics*, 91( 9) (2002) 5858-5866.
- [6] Jones, R., *Mechanics of Composite Materials*, 2nd edition, Taylor & Francis, Philadelphia (Pa.), (1999).



- [7] Maier, M., Experimentelle Untersuchung und numerische Simulation des Crashverhaltens von Faserverbundwerkstoffen. Dissertation, Universität Kaiserslautern, Ludwigshafen, (1990)
- [8] Melo, J., Villena, J., Effect of fiber volume fraction on the energy absorption capacity of composite materials, *Journal of Reinforced Plastics and Composites*, 31(3) (2012) 153-161.
- [9] Morita, H., Adachi, T., Tateishi, Y., Matsumot, H., Characterization of Impact Damage Resistance of CF/PEEK and CF/Toughened Epoxy Laminates under Low and High Velocity Impact Tests, *Journal of Reinforced Plastics and Composites*, 16(2) (1997) 131-143.
- [10] Morye, S. S., Hine, P. J., Duckett, R. A., Carr, D. J., Ward, I. M., Modelling of the energy absorption by polymer composites upon ballistic impact, *Composites Science and Technology*, 60(14) (2000) 2631-2642.
- [11] Muhi, R. J., Najim, F., de Moura, M. F. S. F., The effect of hybridization on the GFRP behavior under high velocity impact, *Composites: Part B*, 40 (2009) 798-803.
- [12] Basalt fabric BBK.2/2.345.100.12 - Twill weave 2/2. Technical data sheet, Incotology Limited, Pulheim, Germany, (2013).
- [13] Carbon fabric twill weave 2/2. Technical data sheet, ECC - Engineered Cramer Composites, Heek, Germany, (2013).
- [14] DIN 65561 Luft- und Raumfahrt; Faserverstärkte Kunststoffe, Prüfung von multidirektionalen Laminaten, Bestimmung der Druckfestigkeit nach Schlagbeanspruchung. Beuth Verlag, Berlin/Heidelberg/New York, (1991).
- [15] [DIN EN ISO 1172 Textilglasverstärkte Kunststoffe; Prepregs, Formmassen und Laminat; Bestimmung des Textilglas- und Mineralfüllstoffgehalts. Beuth Verlag, Berlin, (1998).
- [16] DIN EN 2564 Luft- und Raumfahrt; Kohlenstofffaser-Laminat, Bestimmung der Faser-, Harz- und Porenanteile. Beuth Verlag, Berlin, (1998)
- [17] Epikote Resin 04572 - Anhydrid warm curing epoxy resin. Technical data sheet, Momentive, Columbus OH, (2011).
- [18] Glass fabric Interglas Type 92125 - Twill weave 2/2. Technical data sheet, P-D Interglas Technologies GmbH, Erlbach, Germany, (2013).
- [19] Lantor Soric XF. Technical data sheet, Lantor BV, Veenendaal, Netherlands, (2013)..
- [20] Polyoxymethylen (POM). Technical data sheet, Siegele, Augsburg, Germany, (2013).
- [21] Rosenberg, Z., Dekel, E., Terminal Ballistics, Springer-Verlag, Berlin/Heidelberg/London/New York, (2012).
- [22] Saravanan, D.: Spinning the Rocks – Basalt Fibres. *IE(I) Journal-TX*, 86 (2006) 39-45.
- [23] Schmid, V., Jungbauer, B., Romano, M., Ehrlich, I., Gebbeken, N., Diminution of mass of different types of fibre reinforcements due to thermal load. In: Proceedings of the Applied Research Conference, Nürnberg, (2012) 231-235, doi: 10.2370/9783844010930, In: Mottok, J., Ziemann, O. (Eds.): Applied Research Conference 2012 – ARC 2012. Shaker Verlag, Aachen/Herzogenrath, (2012), doi: 10.2370/9783844010930.
- [24] Schürmann, H., Konstruieren mit Faser-Kunststoff-Verbunden. Springer-Verlag, Berlin/Heidelberg, (2005).
- [25] Witten, E., Handbuch Faserverbundkunststoffe, Grundlagen Verarbeitung Anwendungen. GWV Fachverlag, Wiesbaden, (2010).